Oxygen Isotope Effects as Probes of Electron Transfer Mechanisms and Structures of Activated O_2

JUSTINE P. ROTH*

Department of Chemistry, Johns Hopkins University, 3400 North Charles Street, Baltimore, Maryland 21218

RECEIVED ON JULY 26, 2008

CONSPECTUS

Competitively determined oxygen (^{18}O) isotope effects can be powerful probes of chemical and biological transformations involving molecular oxygen as well as superoxide and hydrogen peroxide. They play a complementary role to crystallography and spectroscopy in the study of activated oxygen intermediates by forging a link between electronic/vibrational structure and the bonding that occurs within ground and transition states along the reaction coordinate. Such analyses can be used to assess the plausibility of intermediates and their catalytic relevance in oxidative processes.

This Account describes efforts to advance oxygen kinetic isotope effects (^{18}O KIEs) and equilibrium isotope effects (^{18}O EIEs) as mechanistic probes of reactive, oxygen-derived species. We focus primarily on transition metal mediated oxidations, outlining both advances over the past five years and current limitations of this approach. Computational methods are now being developed to probe transition states and the accompanying kinetic isotope effects. In particular, we describe the importance of using a full-frequency model to accurately predict the magnitudes as well as the temperature dependence of the isotope effects. Earlier studies have used a "cut-off model," which employs only a few isotopic vibrational modes, and such models tend to overestimate ^{18}O EIEs.

Researchers in mechanistic biological inorganic chemistry would like to differentiate "inner-sphere" from "outer-sphere" reactivity of O_2, a designation that describes the extent of the bonding interaction between metal and oxygen in the transition state. Though this problem remains unsolved, we expect that this isotopic approach will help differentiate these processes. For example, comparisons of ^{18}O KIEs to ^{18}O EIEs provide benchmarks that allow us to calibrate computationally derived reaction coordinates. Once the physical origins of heavy atom isotope effects are better understood, researchers will be able to apply the competitive isotope fractionation technique to a wide range of pressing problems in small molecule chemistry and biochemistry.
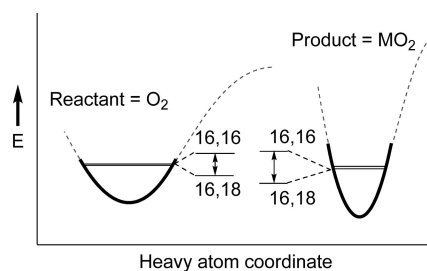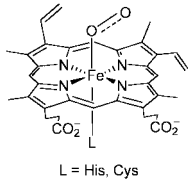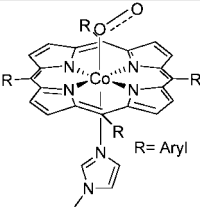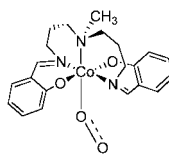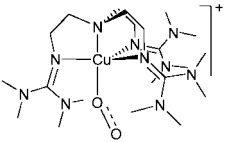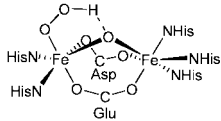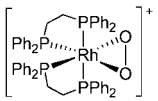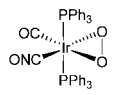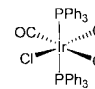
I. Introduction

Reactive intermediates generated from O_2 are among the most challenging to study due to their propensity to react by low-energy pathways. Protein crystallographic and spectroscopic methods have provided valuable insights in systems where metal-activated oxygen intermediates are proposed. Yet with regard to static measurements, it is often difficult to assess whether the observed species are catalytically relevant. Heavy atom isotope effects,[1] specifically on reactions of O_2, com-

plement the above approaches by forging a link between electronic/vibrational structure and the bonding changes that occur along the reaction coordinate.

The analysis of oxygen isotope effects has a long history highlighted by Dole's discovery that ^{18}O is more abundant in the atmosphere ($\%^{18}O = 0.2030$) than in seawater ($\%^{18}O = 0.1999$).[2] This observation, known as the "Dole effect", reflects a multitude of mass-dependent and mass-independent processes. Exposing the origins of both phe-

TABLE 1. ^{18}O EIEs upon Binding of O_2 to Proteins and Inorganic Compounds

Reactant + O_2	Product	^{18}O EIE$_{exp}$[a]	^{18}O EIE$_{calc}$[b]
Fe^{II}-hemoglobin, myoglobin, P450cam	*(porphyrin structure, L = His, Cys)*	1.0039 ± 0.0002 [c] 1.0054 ± 0.0006 [c] 1.0048 ± 0.0006 [d]	0.995 (singlet) 1.0041 (triplet) [e,f]
Co^{II}Por(L)	*(porphyrin structure, R = Aryl)*	1.0028 ± 0.0014 (MeTHF 248 K) [f]	1.0039 (THF, 248 K)[e]
Co^{II}(SMDPT)	*(Co complex structure)*	1.0072 ± 0.0014 [f] (DMF, 294 K) 1.0034 ± 0.0021 (DMF, 218 K) 1.0056 ± 0.0025 (MeTHF, 249 K)	1.0069 (DMF, 294 K)[e] 1.0027 (DMF, 218 K)[e] 1.0043 (THF 249 K)[e]
[Cu^{I}(TMG$_3$Tren)]$^+$	*(Cu complex structure)*	1.0149 ± 0.0012 [g] (DMF, 261 K)	1.0128 [g] (DMF, 261K)
Fe^{II}-hemerythrin	*(diiron complex structure)*	1.0113 ± 0.0005 [c]	1.0115 [h]
[Rh^{I}(dppe)$_2$]$^+$	*(Rh complex structure)*	1.0199 ± 0.0017 (DMF, 298 K) [f]	1.0178[e]
Ir^{I}(PPh$_3$)$_2$(CO)CNO	*(Ir complex structure)*	1.0226 ± 0.0013 (DMF, 298 K) [f]	1.0176[e]
Ir^{I}(PPh$_3$)$_2$(CO)Cl	*(Ir complex structure)*	1.0305 ± 0.0023 (DMF, 298 K) [f]	1.0169[e]

[a] In H_2O at 298 K unless noted; THF = tetrahydrofuran, MeTHF = methyltetrahydrofuran, DMF = *N,N*-dimethylformamide. [b] Calculated using a full frequency model at the experimental temperature in the gas phase unless noted. [c] Reference 6. [d] Reference 38. [e] Reference 26. [f] Reference 24. Calculated for structure with R = H. [g] Reference 27. [h] Reference 31.

nomena remains an important challenge. Deficiencies in our understanding impose limitations on the value of isotope effects in fields ranging from chemistry to the atmospheric, environmental, and biological sciences.

The methodology for determining competitive isotope effects on enzymatic reactions of O_2 has been in place for some time,[3] and there are measurements that date from the 1950s.[4] Early analyses were performed on "water splitting"

during photosynthesis as well as the oxygenase activity of the enzyme rubisco.[5] Mechanistic insights were limited, however, in the absence of benchmarks for differentiating "inner-sphere" and "outer-sphere" electron transfer. These terms refer to the extent to which a bonding interaction develops between a redox metal or organic moiety and O_2 in the transition state.

An early indication that measurements of ^{18}O isotope effects could be useful in probing structures came from the laboratories of Klinman, who applied the technique to the reversible binding of O_2 to metalloproteins.[6] Later studies afforded ^{18}O kinetic isotope effects (KIEs) on reactions of metalloenzymes and more recently on reactions of inorganic molecules.[7−9] Originally, ^{18}O KIEs were used to simply assess the involvement of O_2 in the rate-determining step.[10−14] In later works, comparisons of ^{18}O KIEs to equilibrium isotope effects (EIEs) were used to infer identities of O_2-derived intermediates.[15−19] Similar methods have recently been extended to probe reactions of $O_2^{•−}$ and H_2O_2.[16,20,21]

Much progress toward understanding the origins of ^{18}O EIEs and KIEs has occurred over the past five years, in part due to efforts by the author to study biological and inorganic reactions in parallel.[8,9] Since early works by Bigeleisen[22] and Wolfsberg[23] computational methods for interpreting isotope effects have become more tractable. As will be shown here, density functional theory (DFT) methods have been refined to the point that they can be used to reliably predict ^{18}O EIEs on reactions of O_2.

II. Equilibrium Isotope Effects

A. Experimentation. The first measurements of ^{18}O EIEs were performed on O_2-carrier proteins[6] and followed by proof-of-concept studies using synthetic inorganic compounds.[24] Together these works exposed a correlation between the magnitudes of ^{18}O EIEs and structures containing O_2 bound as an end-on superoxide (O_2^{-I}) and side-on peroxide (O_2^{-II}) ligand. The technique used in these experiments involves analyzing competitive isotope fractionation, that is, the change in $^{18}O/^{16}O$ within the O_2 released from equilibrated solutions. A brief description is provided below with the reader referred elsewhere[7,8] for details concerning instrumentation and methodology.

The parameters determined experimentally include the amount of O_2 taken up by the reduced carrier and the change in $^{18}O/^{16}O$ from natural abundance. For ease of sample handling, O_2 is quantitatively combusted to CO_2 prior to pressure determination and isotope ratio mass spectrometry. The resulting ^{18}O EIE is defined according to eq 1 for the reversible addition of O_2 to form an oxygenated product as in Table 1. The f reflects the fractional change in freely dissolved O_2

concentration upon binding to the reduced O_2-carrier. R_u and R_t correspond to the ratios ($^{18}O/^{16}O$) in the $O_2^{unbound}$ and O_2^{total}, respectively. After equilibration with the atmosphere, $[O_2]^{total}$ = $[O_2]^{unbound} + [O_2]^{bound}$.

$$^{18}O \, EIE = \frac{K(^{16}O^{16}O)}{K(^{16}O^{18}O)} = \frac{1-f}{(R_t/R_u) - f} \qquad (1)$$

B. Calculation of Oxygen Equilibrium Isotope Effects. The formalism of Bigeleisen and Goeppert−Mayer (eq 2)[22] is used to calculate ^{18}O EIEs from gas-phase partition functions corresponding to zero point energy (ZPE), vibrational excitation energy (EXC), and the mass and moments of inertia (MMI). ZPE is typically associated with the isotope effect upon $\Delta H°$ whereas EXC × MMI is associated with the isotope effect upon $\Delta S°$.[25] An isotope exchange reaction (eq 3) is used to define the partition functions (eqs 4−6) in terms of vibrational frequencies of the reactant and product states; here k is Boltzmann's constant, h is Planck's constant, and T is temperature. A is the O_2, and B is the oxygen-derived product. The asterisk designates the site of the ^{18}O.

$$^{18}O \, EIE = ZPE \times EXC \times MMI \qquad (2)$$

$$\underbrace{O_2 + MO_2^*}_{A + B^*} \rightleftharpoons \underbrace{O_2^* + MO_2}_{A^* + B} \qquad (3)$$
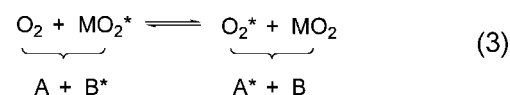
$$ZPE = \frac{\left[\prod_j^{3N-6} \frac{\exp(h\nu_j^{B*}/(2kT))}{\exp(h\nu_j^{B}/(2kT))} \right]}{\left[\prod_i^{3N-5} \frac{\exp(h\nu_i^{A*}/(2kT))}{\exp(h\nu_i^{A}/(2kT))} \right]} \qquad (4)$$

$$EXC = \frac{\left[\prod_j^{3N-6} \frac{1 - \exp\{-(h\nu_j^{B*}/(kT))\}}{1 - \exp\{-(h\nu_j^{B}/(kT))\}} \right]}{\left[\prod_i^{3N-5} \frac{1 - \exp\{-(h\nu_i^{A*}/(kT))\}}{1 - \exp\{-(h\nu_i^{A}/(kT))\}} \right]} \qquad (5)$$

$$MMI = VP = \frac{\prod_j^{3N-6} (\nu_j^{B}/\nu_j^{B*})}{\prod_i^{3N-5} (\nu_i^{A}/\nu_i^{A*})} \qquad (6)$$

When full sets of vibrational frequencies are available, application of the Redlich−Teller product rule allows MMI to be calculated as a vibrational product, VP (eq 6). Theoretically, the result should be the same when computed from the classical expression (eq 7), which contains molecular masses (M)
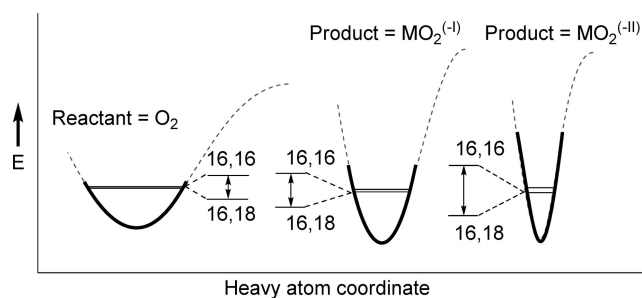
FIGURE 1. Inverse zero point energy effect upon binding of O_2 to a metal center.

and rotational moments of inertia (I). Deviations occur when a truncated set of frequencies is used in the calculations.[26]

$$
MMI = \frac{\left[\left(\frac{M_{16-16}}{M_{16-18}}\right)^{3/2} \prod_{i}^{n_{rot}} \left(\frac{I_{i,16-16}}{I_{i,16-18}}\right)^{1/2}\right]_B}{\left[\left(\frac{M_{16-16}}{M_{16-18}}\right)^{3/2} \prod_{i}^{n_{rot}} \left(\frac{I_{i,16-16}}{I_{i,16-18}}\right)^{1/2}\right]_A} \quad (7)
$$

In Table 1, mostly normal ^{18}O EIEs (>1) are observed reflecting enrichment of ^{18}O in freely dissolved O_2 relative to the product. The apparent trend between the magnitude of ^{18}O EIEs and formal level of O−O bond reduction can be misleading, however, since calculations reveal extensive entropy/enthalpy compensation.[26,27] In this Account, all ^{18}O EIE$_{calc}$ were derived using a full frequency model affording excellent agreement with the experiments, to within ~0.2% (Table 1).

The ZPE calculated from eq 4 is inverse (<1) when O_2 coordinates to a metal. This is somewhat surprising in view of the resultant O−O bond reduction. ZPE becomes more inverse when the total isotopic shift of vibrations within the product, $\sum(\nu^{16,16} - \nu^{16,18})_{prod}$, exceeds the shift of the single stretch in O_2, $\nu^{16,16} - \nu^{16,18}$. In contrast, normal ($>1$) ZPE terms are computed for simple O_2 reduction to $O_2^{\bullet-}$, $HO_2^{\bullet}$ and H_2O_2 (3.4%, 1.0%, and 0.3%); the ^{18}O EIEs vary accordingly from 3.3% to 1.0% to 0.9%. This behavior is opposite to metal−O_2 coordination depicted in Figure 1, where an increased force constant relative to O_2 derives from consideration of the O−O stretch, metal−oxygen vibrations, and any other modes sensitive to ^{18}O substitution within the product.

The new isotopic bonds formed upon coordinating O_2 to a metal center also give rise to an inverse EXC. In general, the EXC (eq 5) is more inverse for end-on superoxide structures than for side-on peroxide structures, while the opposite is true for the ZPE. For exact values, the reader is referred to the primary literature.[15,26,27] The inverse EXC is attributed to the greater population of vibrational energy levels, which are more closely spaced in the heavier isotopologue than in the
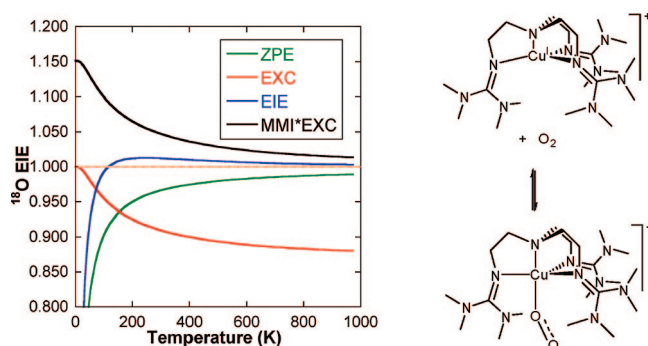
FIGURE 2. Calculated ^{18}O EIEs for formation of a Cu(η^1-O_2)TMG$_3$Tren.[27]

light one. EXC becomes more inverse approaching 1/MMI at the limit of infinite temperature. At this limit, all vibrational levels are equally populated and EXC × MMI = 1. Under the same conditions of increasing temperature the ZPE varies as a negative exponential approaching 1.

For small molecule activation, the inverse EXC is offset by a large normal MMI (~1.15). The temperature independent MMI term reflects loss of mass-dependent rotational and translational modes when O_2 binds to the heavy metal fragment. This effect is offset by the formation of new low-frequency bonds. The product, EXC × MMI, reflecting the isotope effect on $\Delta S°$ is large and normal as opposed to the inverse ZPE, representing the isotope effect on $\Delta H°$. Similar behavior has been noted by Parkin et al. for addition of H_2 to transition metal complexes,[25] where the isotope effect upon $\Delta S°$ causes deviation from a normal linear van't Hoff plot. Such behavior is depicted for O_2 binding to copper(I) in Figure 2 where the ^{18}O EIE arises from compensating enthalpic (ZPE) and entropic (EXC × MMI) effects.

^{18}O EIEs can be similar for intermediates derived from inorganic compounds and metalloproteins. The primary influences are electron density at the metal and its propensity to form strong bonds to O_2. As a result, ^{18}O EIEs have been observed to be up to a factor of 8 (!) larger for side-on (η^2) peroxide structures than for end-on (η^1) superoxide structures.[24] The larger ^{18}O EIEs associated with η^2-peroxide comes from a less inverse EXC contribution reflecting stronger, higher frequency metal−oxygen bonds. The MMI is relatively constant for all O_2 binding reactions making EXC × MMI larger than that for the η^1-superoxide structures. As described above, EXC × MMI offsets the ZPE, which is more inverse for η^2- peroxide than η^1-superoxide structures.[15,17,26] Since EXC × MMI actually makes the ^{18}O EIE > 1, this contribution may be viewed as the primary determinant of the normal ^{18}O isotope effect, which would be inverse if based solely on ZPE considerations.

Differences in [18]O EIEs are less clear-cut when comparing O_2 complexes of different metals with variable coordination geometries. These factors impact the strength of the metal−oxygen bonds. This observation is in line with the bonding interactions appearing similar for six-coordinate Fe(η^1-O_2) and Co(η^1-O_2) complexes where calculated and experimental [18]O EIEs are ca. 0.5‰ at 298 K. We note that in the former, it is difficult to accurately calculate the relevant spin state.[26,27] Though the Fe(η^1-O_2) porphyrin species in globins engage in hydrogen bonding, this effect does not appear to significantly perturb the [18]O EIE as suggested by calculations[26] and experiments with a biomimetic cobalt analogue.[24] The [18]O EIEs for Cu(η^1-O_2) species, some of which are only calculated and not shown in Table 1, are typically larger (0.9−1.3‰)[15,27] than those for Fe(η^1-O_2) and Co(η^1-O_2), which imply more dioxygen-like structures.

Earlier estimates of [18]O EIEs for Cu(η^1-O_2) species as large as 1.6‰ should be viewed as conservative upper limits. This situation derives from the uncertainty in extracting [18]O EIEs from multistep mechanisms where the KIE contribution from the rate-limiting step is ambiguous.[20] Moreover, CuO_2 species with the same formal oxidation states have been described in terms of a valence bond continuum,[28] with structures ranging from oxygen-like to superoxide-like to peroxide-like. The computed [18]O EIEs of 2.3−3.1‰ reproduce these trends expected for the Cu(η^2−O_2) coordination geometry.[15,27] The larger [18]O EIEs again be traced to less inverse EXC terms, which result in a larger entropic contribution to the [18]O EIE through MMI × EXC.

Stretching frequencies have often been used to indicate the level of O−O reduction within metal−O_2 complexes.[29] The ν_{O-O} values for superoxide structures invariably fall within 1100−1300 cm^{-1}, while ν_{O-O} values for peroxide structures are within 800−950 cm^{-1}. Since the [18]O EIE is determined by all isotopic vibrations of the product, it complements the spectroscopic observation of a few specific modes above 300 cm^{-1}. In addition to the magnitude of the [18]O EIE, its temperature dependence is also a distinguishing factor. Maxima occur at higher temperatures for η^1-superoxide structures than for η^2-peroxide structures, due to differing contributions from low frequency modes (cf. Figure 2).[26,27]

C. Full Frequency versus Cut-off Models. In earlier studies, heavy atom EIEs were interpreted in terms of bond order changes by analogy with secondary isotope effects. Since methods for calculating optimized geometries and molecular force fields were not readily available, [18]O EIEs on reactions of O_2 were estimated using "cut-off" models.[7,23] In these models, only a few, sometimes arbitrarily chosen, isotopic vibra-
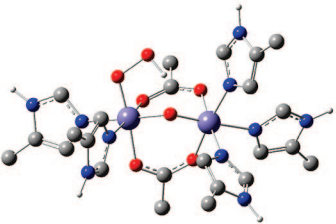
tions were analyzed. Stern and Wolfsberg[30] originally proposed this type of analysis for "large molecules" in the high-temperature limit. It was further noted that the requisite cancellation of terms would be most reliable when similar vibratonal frequencies were omitted in the reactant and product states. With regard to O_2-binding, the omissions are necessarily dissimilar with only the product frequencies being left out of the calculations. It follows that the application of cut-off models to reactions of O_2 may be inherently flawed. Within this approach, the [18]O EIEs are overestimated, as discussed in a recent review,[9] and should be viewed as upper limits.

In other interpretations of [18]O EIEs and KIEs, the analogy has been made between a metal and a proton. For example, equating the heme-derived Fe(η^1-O_2) to HO_2• emphasizes the contribution from the change in O−O force constant.[6] This type of analysis is clearly an oversimplification because it neglects the compensating enthalpic and entropic effects, which, as described above, are characteristic of small molecule binding to transition metals.

More recent studies[16,26,27] have focused on refining DFT methods such that they provide full sets of reliable vibrational frequencies for the reactant as well as product states; the latter are unavailable from even the best spectroscopic experiments. Surprisingly, some common DFT methods fail to reproduce the bond length and stretching frequency associated with the isotopologues of O_2. Thus, care must be taken to choose the appropriate basis sets and functional. As demonstrated in Table 1, agreement with experimental [18]O EIEs at varying temperatures is excellent (±0.2‰) when the calibrated *m*PWPW91 functional is applied to O_2 as well as first and second row transition metal complexes.[26,27] Solvent corrections can enhance the agreement within the limits of error. Poorer performance is noted for third row transition metals; this is likely due to insufficient basis functions and the difficulty in obtaining optimized structures with accurate force fields.

Full frequency calculations, which employ isotopic vibrations from appropriately calibrated DFT methods yield results that are more reliable than the cut-off models. A case in point is oxyhemerythrin where the [18]O EIE is grossly overestimated when only the observed stretching frequencies associated with the ν(Fe−O), ν_{as}(Fe−O), ν(Fe−O_2H), and ν(O−OH) are used in the calculations.[9] Yet when the DFT method is employed with tight constraints on geometry optimization, the calculated vibrational frequencies predict an [18]O EIE$_{calc}$ of 1.15‰.[31] This value is in excellent agreement with the experimental [18]O EIE of 1.13‰.[6] Notably the DFT calculations predict the frequency

TABLE 2. Analysis of the Oxygen Isotope Effect for O_2 Binding to Hemerythrin

Low spin oxyhemerythrin model [a]	Fe^{16}O^{16}OH vs.	ZPE	EXC	MMI [b]	EIE$_{calc}$
	Fe^{16}O^{18}OH	0.9308	0.9401	1.1523	1.0084
	Fe^{18}O^{16}OH	0.9618	0.9158	1.1519	1.0147
	Ave	0.9461	0.9278	1.1521	1.0115

[a] Acetate was used for aspartate and glutamate and methylimidazole for histidine; $S = 0$ arises from antiferromagnetic coupling of the iron centers. [b] Equation 6.

of the hydrogen-bonded terminal O−H for the low-spin state ($v(^{16}$O−H$) = 2564.0$, $v(^{18}$O−H$) = 2555.4$) to be significantly down-shifted relative to an isolated $v(^{16}$O−H$) = 3539$, $v(^{18}$O−H$) = 3527$,[17] thus making a significant difference in the computed ^{18}O EIE. The analysis in Table 2 indicates no need for scaling frequencies or making allowance for the intramolecular isotope effect reflecting preferential coordination of ^{18}O to Fe or ^{16}O to H.

III. Competitive Oxygen Kinetic Isotope Effects (^{18}O KIEs)

Similar to ^{18}O EIEs, ^{18}O KIEs can be determined to high precision using competitive methodology and natural abundance O_2.[7,8] Catalytic and stoichiometric reactions are analyzed according to eq 8 where the KIE is derived from the ratio of oxygen isotopes in the residual O_2, that is, ^{18}O/^{16}O(R_f), relative to the initial ^{18}O/^{16}O(R_0) in the starting material. The fractional conversion (f) also factors into the expression, which has two familiar forms:

$$^{18}\text{O KIE} = \frac{k(^{16}\text{O}^{16}\text{O})}{k(^{16}\text{O}^{18}\text{O})} = \left[1 + \frac{\ln(R_f/R_o)}{\ln(1-f)}\right]^{-1} = \frac{\ln(1-f)}{\ln(1-f)(R_f/R_0)}$$

(8)

The experimental methodology developed for O_2 has since been extended to superoxide ($O_2^{\bullet-}$)[20,21] and hydrogen peroxide (H_2O_2).[16] Comparative measurements can be informative when similar intermediates are generated from different oxidants. The observed ^{18}O KIEs can be related by considering the theoretical ^{18}O EIEs (quoted above for reduction of O_2 to $O_2^{\bullet-}$ or H_2O_2). The competitive ^{18}O KIE is by definition an isotope effect on a second-order process, reflecting all steps beginning with encounter leading up to and including the first kinetically irreversible step. Thus, measurements where common reactive intermediates are generated from H_2O_2 and O_2 may complement one another or expose kinetic complexity that would otherwise be difficult to detect.

Proof-of-concept studies, which illuminate the physical origins of ^{18}O KIEs on reactions of O_2, are needed to progress further toward identification of reactive intermediates. This is a challenging problem due to the largely entropic nature of the reaction barrier. At present, constructing boundary conditions for ^{18}O KIEs is precluded by uncertainties concerning transition state structure, reaction coordinate frequency and, more generally, the mechanism of electron transfer (ET) to O_2. Inner-sphere and outer-sphere ET mechanisms are defined with regard to the presence of a bond to O_2 in the transition state.

While ^{18}O EIEs have often been assumed to represent upper limits for ^{18}O KIEs in mechanistic studies,[7−21] this relationship has not been rigorously examined for a variety of reactions. *For instance, it is unknown to what extent the reaction coordinate depends on oxygen isotope in reactions where a metal−O_2 adduct is reduced by electron or hydrogen atom transfer.* Cases illustrating current limitations in understanding these issues are presented below.

A. Outer-Sphere Electron Transfer (ET). ^{18}O KIEs upon outer-sphere ET to O_2 have been described within the context of Marcus theory.[19] Isotope substitution can influence $\Delta G°$, estimated from redox potentials, as well as the O−O bond reorganization energy, defined classically as λ_{in} or in terms of quantum mechanical Franck−Condon overlap factors.[32,33] Isotope effects on these parameters have been estimated for the self-exchange reaction: $^*O_2 + O_2^{\bullet-} \rightarrow {}^*O_2^{\bullet-} + O_2$.[19] Since the normal mode stretching frequencies (v_{O-O}) of O_2 and $O_2^{\bullet-}$ exceed thermal energy ($>4kT$), the reaction is more correctly treated within the quantum limit, in terms of Franck−Condon overlap factors. These overlap factors,
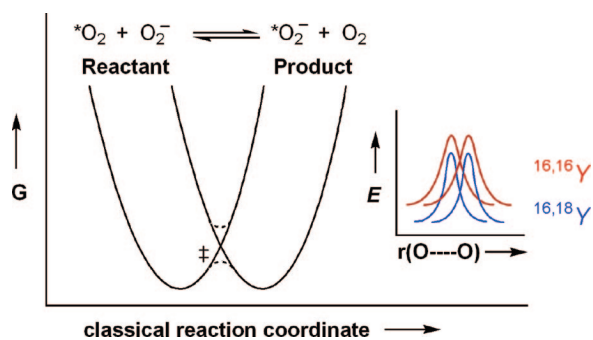
FIGURE 3. Quantum mechanical model for the ^{18}O KIE on $O_2/O_2^{\bullet-}$ self-exchange.

denoted Y, are defined from the isotopic ν_{O-O}, reduced masses and bond lengths, $r(O-O)$, of the reactant and product (Figure 3).

^{18}O KIEs upon outer-sphere ET to O_2 have been found to fall within a narrow range of 2.6–2.8% when $\Delta G°$ is close to 0.[19] Experiments have been performed using glucose oxidase, a flavoenzyme where only an outer-sphere pathway is plausible.[18] The observed ^{18}O KIEs are in agreement with the quantum mechanical formalism of Jortner, which attributes the isotope effect to differences in vibrational wave function overlap at the classically defined transition state (Figure 3) rather than the effects of $\Delta G°$.[32,33]

A shortcoming of the above approach is that it assumes an averaged force constant for the reactant (O_2) and product ($O_2^{\bullet-}$) states and thus, does not account simultaneously for the change in force constant, i.e. the ^{18}O EIE. Another uncertainty concerns the variation in ^{18}O KIE with $\Delta G°$. It follows from the basic Marcus equation, $\Delta G^{\ddagger} = \lambda/4(1 + \Delta G°/\lambda)^2$, and the definition ^{18}O KIE $= \exp[(^{16,18}\Delta G^{\ddagger} - {}^{16,16}\Delta G^{\ddagger})/(RT)]$ that the maximum ^{18}O KIE should occur at $\Delta G° = 0$ kcal mol^{-1} and should vary parabolically to a minimum of 1 when $|\Delta G°| = \lambda$.

Though the Jortner model has been applied in mechanistic studies of ET to O_2,[21] more advanced descriptions are needed to predict the behavior of ^{18}O KIEs when $\Delta G°$ is very favorable or very unfavorable. In these cases, excited-state vibrations are likely to contribute differently to the rates of the two isotopologues. A vibronic model derived from Marcus theory and popularized for proton-coupled electron transfer[34] may be useful in this respect because it explicitly considers the ^{18}O EIE as well as contributions from ground and excited vibrational energy levels.

B. Inner-Sphere Electron Transfer. The interpretation of ^{18}O KIEs is perhaps most challenging for reactions where O_2 coordinates to a reduced metal center. In these cases, defining a stable saddle point along the reaction coordinate is critical. It follows from transition-state theory (TST), that the ^{18}O

KIE can be expressed according to eq 9. The ν_{RC} is the reaction coordinate frequency and K_{TS} is a pseudoequilibrium constant for interconverting the reactant and transition state. Isotopic partition functions associated with K_{TS} are defined analogously to the ^{18}O EIE (eq 10) with the exception that VP (cf. eq 6) has one less mode due to converting a translation to a vibration in the transition state.

$$^{18}O\,KIE_{calc} = \left(\frac{^{16,16}\nu_{RC}}{^{16,18}\nu_{RC}}\right)\left(\frac{^{16,16}K_{TS}}{^{16,18}K_{TS}}\right) \quad (9)$$

$$K_{TS} = VP \times EXC \times ZPE \quad (10)$$

Transition states for bimolecular reactions of O_2 can be difficult to calculate because of the large contribution from entropy to the free energy barrier.[35] For this reason, variational TST methods may be worth investigating. Some computational studies of bimolecular O_2 reactions have reported stable saddle-point structures, which correspond to unimolecular rearrangements subsequent to O_2 coordination to the metal.[36] Such rearrangements have been proposed to accompany spin-state change,[36] as well as ligand dissociation.[35] The analyses of ^{18}O KIEs on such irreversible O_2 binding reactions have the added complexity that combination metal–O and O–O vibrational modes may define the reaction coordinate. A major question, therefore, concerns the isotope sensitivity of ν_{RC} and its contribution to the overall ^{18}O KIE in eq 9. A significant isotope effect on ν_{RC} could negate the commonly made assumption that the ^{18}O EIE is the upper limit to the ^{18}O KIE.[7–15,17–20,37,38]

Experiments have been conducted on irreversible O_2 binding reactions, which form side-on peroxide compounds analogous to those in Table 1. In this study,[37] the ^{18}O KIEs were found to vary from 0.69% to 2.68%, all falling within the ^{18}O EIEs estimated from cut-off models. Though further work is needed to corroborate the ^{18}O EIEs through experiment and with DFT methods,[26] a large ν_{RC} contribution, in excess of 0.6% would be difficult to reconcile with the results.[8,37] In addition, different reactions should be analyzed to determine the generality of these observations. There are bound to be cases where O_2 reduction occurs by a multistep process[36] possibly resulting in a significant contribution of the O–O stretch to ν_{RC}. For instance, recent studies of ^{18}O EIEs on H_2O_2 activation suggest large isotope effects deriving from the ν_{RC}.[16]

C. Implications for Enzymatic Reactions. A deeper understanding of ^{18}O isotope effects has important ramifications for understanding oxidation mechanisms in chemistry and biology. In order to better utilize these mechanistic probes, some issues still need to be resolved including: (i) the
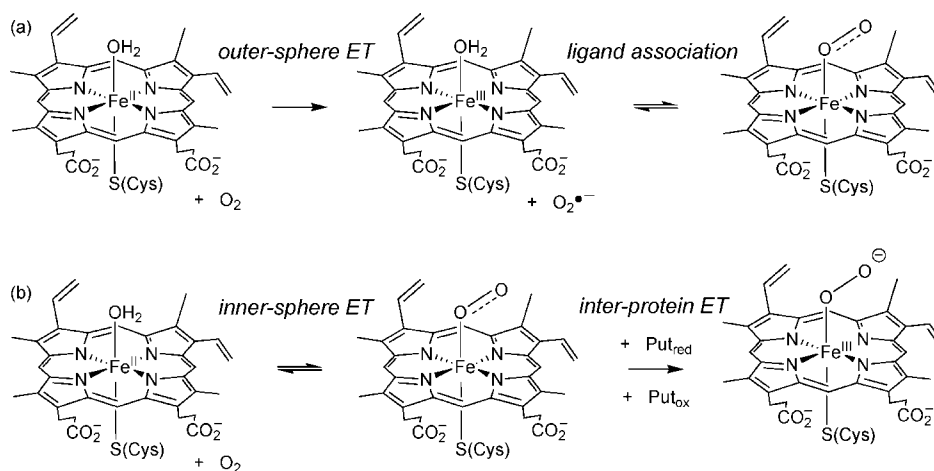
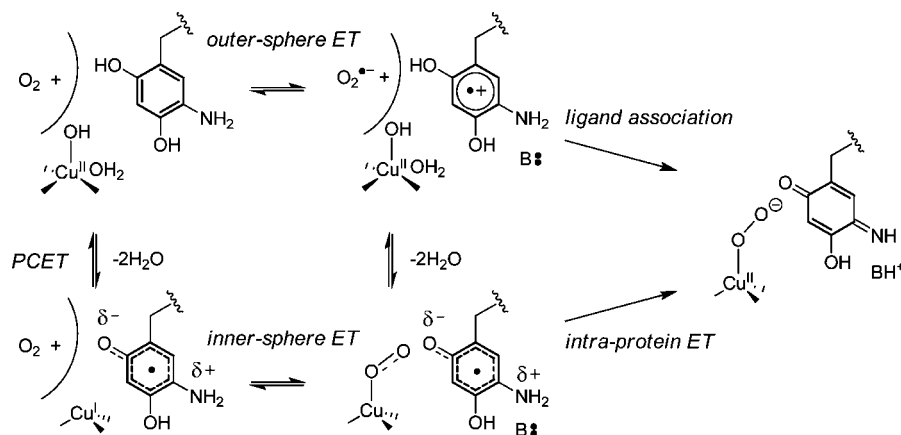FIGURE 4. Proposed mechanisms for ET in cytochrome P450$_{cam}$.

FIGURE 5. Inner- and outer-sphere ET in copper amine oxidase.

relationship of the ^{18}O KIE to EIE for different types of O_2 activation reactions and (ii) the influences of $\Delta G°$ on transition state structures.

In recent studies of a cytochrome P450 enzyme, P450$_{cam}$, the ^{18}O KIE upon O_2 consumption during catalysis was compared with the ^{18}O EIE upon reversible O_2 binding to the reduced enzyme. The studies aimed to address the mechanism by which the reduced heme was reoxidized during catalysis.[38] Purdy et al. demonstrated an ^{18}O KIE of 1.47%, which significantly exceeded the ^{18}O EIE of 0.48% corresponding to formation of the Fe(η^1-O_2) complex. On the basis of this comparison and the assumption that the ^{18}O KIE is limited by the ^{18}O EIE, an inner-sphere mechanism was rejected and a rate-determining outer-sphere ET mechanism was proposed. This step was suggested to precede rapid binding of $O_2^{\bullet-}$ to the ferric enzyme. An alternative mechanism where O_2 binds followed by rate-determining interprotein ET from reduced putidaredoxin could not be excluded, however, in light of the ^{18}O KIE. The mechanisms predict rate-determining formation of different intermediates, as depicted in Figure 4. Yet the magnitude of the ^{18}O KIE does not distinguish one from the other.

A similar argument is encountered in studies of copper amine oxidases. These enzymes use Cu^{II} and a tyrosine-derived topaquinone cofactor to convert primary amines (RCH$_2$NH$_2$) to aldehydes (RCHO) and NH$_3$ while reducing O_2 to H$_2$O$_2$. During the oxidative half-reaction, ^{18}O KIEs similar in magnitude to those seen in cytochrome P450$_{cam}$ are observed and have been tentatively attributed to rate-determining outer-sphere ET. This proposal[13,14] has been challenged on the basis of experimental/computational studies, which found that formation of a Cu(η^1-O_2) intermediate is also consistent with observations.[15] Assignment of the O_2-reactive species in the copper amine oxidases is complicated due to a rapid internal proton coupled electron transfer (PCET), which interconverts Cu^{II} and Cu^{I} together with the fully reduced aminoquinol (TPQ$_{red}$) and the semiquinone (TPQ$_{sq}$) in Figure 5. The Cu^{I}/TPQ$_{sq}$ is predisposed to react by an inner-sphere ET pathway whereas the Cu^{II}/TPQ$_{red}$ may react by outer-sphere ET.

The reduced copper amine oxidase from *Hansenula polymorpha* (HPAO) is dominated by the Cu^{II}/TPQ$_{red}$ enzyme form. It has been shown that Co^{II} can be substituted for Cu^{II} with k_{cat} remaining unchanged.[39] This behavior implies that O_2 reduc-

tion is mediated by the TPQ_{red} and that the metal has a spectator or electrostatic role. An outer-sphere ET mechanism was proposed and later substantiated by studies of the single-turn-over reaction.[40] These stopped-flow experiments revealed saturation kinetics, which was attributed to noncovalent binding of O_2 to the protein. Further, the steady-state k_{cat} was suggested to be ~30% rate limited by the initial ET step. HPAO exhibits an ^{18}O KIE = 1.0%, which decreases to 0.75% in a faster reacting D630N mutant where more of the Cu^I/TPQ_{sq} accumulates, suggesting the possibility of kinetic complexity.[41] As observed with cytochrome P450$_{cam}$, the deviation of ^{18}O KIEs from values of 2.6−2.8% expected for outer-sphere electron transfer[19] have been difficult to explain.[9]

In contrast to HPAO, the amine oxidase from pea seedling (PSAO) exists predominantly (~80%) in the Cu^I/TPQ_{sq} form.[15] Rapid PCET equilibrates the Cu^I and Cu^{II} forms making either kinetically competent for catalysis.[42] Analysis of the thermodynamics for inner- and outer-sphere ET pathways (Figure 5) indicates that the Cu^I/TPQ_{sq} should react with O_2 more readily than the Cu^{II}/TPQ_{red}, the latter cofactor in its neutral state. On the basis of steady-state experiments, which implicate an intermediate prior to the first irreversible step in O_2 consumption, PSAO has been proposed to react by rate-limiting reduction of a $Cu(\eta^1\text{-}O_2)$ complex.[15]

Consistent with the proposed mechanism, the ^{18}O KIE = 1.36% in PSAO is larger than the computed ^{18}O EIE of 0.92−0.95% for pre-equilibrium formation of the structurally relevant $Cu(\eta^1\text{-}O_2)$[43] and smaller than ^{18}O EIEs of 2.14−1.78% calculated for the expected copper(II) peroxide or hydroperoxide product.[15] Further, the ^{18}O KIE is likely an intrinsic value as there are no signs of kinetic complexity upon varying the reaction temperature or pH nor is there an observable solvent KIE indicating the absence of proton transfer. The magnitude of the ^{18}O KIE, therefore, should reflect the position of the transition state for electron transfer between superoxo- and peroxo-like, as determined by the reaction driving force. For large reorganization energies small variations in KIE may result.

For copper amine oxidases, there is still debate regarding the mechanism of ET and whether the formation of the $Cu(\eta^1\text{-}O_2)$ intermediate occurs in one or two steps.[9] This problem of differentiating inner-sphere from outer-sphere ET mechanisms is analogous to that in cytochrome P450$_{cam}$. The issue can be traced back to the importance of understanding how $\Delta G°$ affects transition state structure in all types of electron transfer and consequently the magnitude of the intrinsic ^{18}O KIE. Once this problem is sorted out, the mechanistic ambiguities are likely to disappear.

IV. Summary and Future Directions

Competitive isotope fractionation measurements can be performed in different types of laboratories to study mechanisms of small molecule activation. A number of experimental methods are in place for the study of O_2 activation as well as reactions of $O_2^{\bullet-}$ and H_2O_2. The basic methods can be extended to other small molecules including NO, N_2, CO_2, ethylene, etc.

Over the past few years, the physical origins of isotope effects upon metal-mediated O_2 activation have become clearer due to studies of structurally defined inorganic molecules and benchmarked DFT calculations. Computational methods are now being developed to probe transition states and the accompanying kinetic isotope effects.

To advance further in this field, it will be essential to elucidate the relationship between kinetic and equilibrium isotope effects upon different types of O_2 activation reactions as well as the influences of driving force on transition state structure. Once these issues are resolved, ^{18}O KIEs can be used more effectively to probe the reactivity of O_2-derived intermediates in chemical and biological catalysis.

BIOGRAPHICAL INFORMATION

Justine Roth received a B.S. from the University of Florida and a Ph.D. from the University of Washington working with James Mayer. Following that, she was a NIH Postdoctoral Fellow at the University of California, Berkeley, in the laboratories of Judith Klinman. Appointed Assistant Professor of Chemistry at Johns Hopkins University in 2003, her research interfaces biological, inorganic, and physical approaches to elucidate mechanisms of oxidation reactions.

FOOTNOTES

*Phone: 410-516-7835. Fax: 410-516-8420. E-mail: jproth@jhu.edu.

REFERENCES

1 Cleland, W. W. Isotope effects: Determination of enzyme transition state structure. *Methods Enzymol.* **1995**, *249*, 341–373.

2 Dole, M. The natural history of oxygen. *J. Gen. Physiol.* **1965**, *49*, 5–27.

3 Cahill, A. E.; Taube, H. The use of heavy oxygen in the study of reactions of hydrogen peroxide. *J. Am. Chem. Soc.* **1952**, *74*, 2312–2318.

4 Feldman, D. E., Jr.; Benson, B. E. Oxygen isotope fractionation in reactions catalyzed by enzymes. *Science* **1959**, *129*, 146–147.

5 Guy, R. D.; Fogel, M. L.; Berry, J. A. Photosynthetic fractionation of the stable isotopes of oxygen and carbon. *Plant Physiol.* **1993**, *101*, 37–47.

6 Tian, G.; Klinman, J. P. Discrimination between ^{16}O and ^{18}O in oxygen binding to the reversible oxygen carriers hemoglobin, myoglobin, hemerythrin, and hemocyanin: A new probe for oxygen binding and reductive activation by proteins. *J. Am. Chem. Soc.* **1993**, *115*, 8891–8897.

7 Roth J. P.; Klinman J. P. *Isotope Effects in Chemistry and Biology*; Kohen, A., Limbach, H.-H., Eds.; CRC Press: Boca Raton, FL, 2006; pp 645−666.

8   Smirnov, V. V.; Brinkley, D. W.; Lanci, M. P.; Karlin, K. D.; Roth, J. P. Probing metal-mediated O_2 activation in chemical and biological systems. *J. Mol. Catal. A: Chem.* **2006**, *251*, 100–107.

9   Roth, J. P. Advances in studying bioinorganic reaction mechanisms: isotopic probes of activated oxygen intermediates in metalloenzymes. *Curr. Opin. Chem. Biol.* **2007**, *11*, 142–150.

10 Tian, G.; Berry, J. A.; Klinman, J. P. Oxygen-18 kinetic isotope effects in the dopamine β-monooxygenase reaction: Evidence for a new chemical mechanism in non-heme, metallomonooxygenase. *Biochemistry* **1994**, *33*, 226–234.

11 Francisco, W. A.; Blackburn, N. J.; Klinman, J. P. Oxygen and hydrogen isotope effects in an active site tyrosine to phenylalanine mutant of peptidylglycine α-hydroxylating monooxygenase: Mechanistic implications. *Biochemistry* **2003**, *42*, 1813–1819.

12 Stahl, S. S.; Francisco, W. A.; Merkx, M.; Klinman, J. P.; Lippard, S. J. Oxygen kinetic isotope effects in soluble methane monooxygenase. *J. Biol. Chem.* **2001**, *276*, 4549–4553.

13 Su, Q.; Klinman, J. P. Probing the mechanism of proton coupled electron transfer to dioxygen: The oxidative half-reaction of bovine serum amine oxidase. *Biochemistry* **1998**, *37*, 12513–12525.

14 Mills, S. A.; Goto, Y.; Su, Q.; Plastino, J.; Klinman, J. P. Mechanistic comparison of the cobalt-substituted and wild-type copper amine oxidase from *Hansenula polymorpha*. *Biochemistry* **2002**, *41*, 10577–10584.

15 Mukherjee, A.; Smirnov, V. V.; Lanci, M. P.; Brown, D. E.; Shepard, E. M.; Dooley, D. M.; Roth, J. P. Inner-sphere mechanism for molecular oxygen reduction catalyzed by copper amine oxidases. *J. Am. Chem. Soc.* **2008**, *130*, 9459–9473.

16 Roth, J. P.; Cramer, C. J. Direct examination of H_2O_2 activation by a heme peroxidase. *J. Am. Chem. Soc.* **2008**, *130*, 7802–7803.

17 Mirica, L. M.; McCusker, K. P.; Munos, J. W.; Liu, H.; Klinman, J. P. 18O kinetic isotope effects in non-heme iron enzymes: Probing the nature of Fe/O_2 intermediates. *J. Am. Chem. Soc.* **2008**, *130*, 8122–8123.

18 Roth, J. P.; Klinman, J. P. Catalysis of electron transfer during activation of O_2 by the flavoprotein glucose oxidase. *Proc. Natl. Acad. Sci. U.S.A.* **2003**, *100*, 62–67.

19 Roth, J. P.; Wincek, R.; Nodet, G.; Edmondson, D. E.; McIntire, W. S.; Kl inman, J. P. Oxygen isotope effects on electron transfer to O_2 probed using chemically modified flavins bound to glucose oxidase. *J. Am. Chem. Soc.* **2004**, *126*, 15120–15131.

20 Smirnov, V. V.; Roth, J. P. Evidence for $Cu-O_2$ intermediates in superoxide oxidations by biomimetic copper(II) complexes. *J. Am. Chem. Soc.* **2006**, *128*, 3683–3695.

21 Smirnov, V. V.; Roth, J. P. Mechanisms of electron transfer in catalysis by copper zinc superoxide dismutase. *J. Am. Chem. Soc.* **2006**, *128*, 16424–16425.

22 Bigeleisen, J. In *Isotope Effects in Chemistry and Biology*; Kohen, A., Limbach, H.-H., Eds.; CRC Press: Boca Raton, FL, 2005; pp 1–39.

23 Wolfsberg, M. In *Isotope Effects in Chemistry and Biology*; Kohen, A., Limbach, H.-H., Eds.; CRC Press: Boca Raton, FL, 2005; pp 89–117.

24 Lanci, M. P.; Roth, J. P. Oxygen isotope effects upon reversible O_2-binding reactions: Characterizing mononuclear superoxide and peroxide structures. *J. Am. Chem. Soc.* **2006**, *128*, 16006–16007.

25 Janak, K. E.; Parkin, G. Experimental evidence for a temperature dependent transition between normal and inverse equilibrium isotope effects for oxidative addition of H_2 to Ir(PMe$_2$Ph)$_2$(CO)Cl. *J. Am. Chem. Soc.* **2003**, *125*, 13219–13224.

26 Smirnov, V. V.; Lanci, M. P.; Roth, J. P. Computational modeling of oxygen isotope effects on metal-mediated O_2 activation at varying temperatures *J. Phys. Chem. A (Wolfsberg Festschrift)* **2009**, ASAP.

27 Lanci, M. P.; Smirnov, V. V.; Cramer, C. J.; Gauchenova, E. V.; Sundermeyer, J.; Roth, J. P. Isotopic probing of molecular oxygen activation at copper(I) sites. *J. Am. Chem. Soc.* **2007**, *129*, 14697–14709.

28 Cramer, C. J.; Tolman, W. B. Mononuclear $Cu-O_2$ complexes: Geometries, spectroscopic properties, electronic structures, and reactivity. *Acc. Chem. Res.* **2007**, *40*, 601–608.

29 Cramer, C. J.; Tolman, W. B.; Theopold, K. H.; Rheingold, A. L. Variable character of $O-O$ and $M-O$ bonding in side-on (h2) 1:1 metal complexes of O_2. *Proc. Natl. Acad. Sci. U.S.A.* **2003**, *100*, 3635–3640.

30 Stern, M. J.; Wolfsberg, M. Simplified procedure for the theoretical calculation of isotope effects involving large molecules. *J. Chem. Phys.* **1966**, *45*, 4105–4124.

31 Supporting Information of ref 16.

32 Buhks, E.; Bixon, M.; Jortner, J.; Navon, G. Quantum effects on the rates of electron-transfer reactions. *J. Phys. Chem.* **1981**, *85*, 3759–3762.

33 Buhks, E.; Bixon, M.; Jortner, J. Deuterium isotope effects on outer-sphere electron-transfer reactions. *J. Phys. Chem.* **1981**, *85*, 3763–3766.

34 Hammes-Schiffer, S. Theoretical perspectives on proton-coupled electron transfer reactions. *Acc. Chem. Res.* **2001**, *34*, 273–281.

35 Aboelella, N. W.; Kryatov, S. V.; Gherman, B. F.; Brennessel, W. W.; Young, V. G., Jr.; Sarangi, R.; Rybak-Akimova, E. V.; Hodgson, K. O.; Hedman, B.; Solomon, E. I.; Cramer, C. J.; Tolman, W. B. Dioxygen activation at a single copper site: structure, bonding, and mechanism of formation of 1:1 Cu-O_2 adducts. *J. Am. Chem. Soc.* **2004**, *126*, 16896–16911.

36 Popp, B. V.; Wendlandt, J. E.; Landis, C. R.; Stahl, S. S. Reaction of molecular oxygen with an NHC-coordinated Pd^0 complex: Computational insights and experimental implications. *Angew. Chem., Int. Ed.* **2007**, *46*, 601–604.

37 Lanci, M. P.; Brinkley, D. B.; Stone, K. L.; Smirnov, V. V.; Roth, J. P. Structures of transition states in metal-mediated O_2 activation reactions. *Angew. Chem., Int. Ed.* **2005**, *44*, 7273–7276.

38 Purdy, M. M.; Koo, L. S.; Ortiz de Montellano, P. R.; Klinman, J. P. Mechanism of O_2 activation by cytochrome P450$_{cam}$ studied by isotope effects and transient state kinetics. *Biochemistry* **2006**, *45*, 15793–15806.

39 Mills, S. A.; Klinman, J. P. Evidence against reduction of Cu^{2+} to Cu^+ during dioxygen activation in a copper amine oxidase from yeast. *J. Am. Chem. Soc.* **2000**, *122*, 9897–9904.

40 Takahashi, K.; Klinman, J. P. Relationship of stopped flow to steady state parameters in the dimeric copper amine oxidase from *Hansenula polymorpha* and the role of zinc in inhibiting activity at alternate copper-containing subunits. *Biochemistry* **2006**, *45*, 4683–4694.

41 Welford, R. W. D.; Lam, A.; Mirica, L. M.; Klinman, J. P. Partial conversion of *Hansenula polymorpha* amine oxidase into a "plant" amine oxidase: Implications for copper chemistry and mechanism. *Biochemistry* **2007**, *46*, 10817–10827.

42 Dooley, D. M.; McGuirl, M. A.; Brown, D. E.; Turow ski, P. N.; McIntire, W. S.; Knowles, P. F. A copper(I)-semiquinone state in substrate-reduced amine oxidases. *Nature* **1991**, *349*, 262–264.

43 Although the ^{18}O KIE for PSAO is comparable to the ^{18}O EIE determined for Cu(η^1-O_2)TMG$_3$Tren (cf. Table 1) variations are expected due to coordination geometry and electron density at copper.